B0620

Chemical and structural stability of $SrTiO_3$-based materials under SOFC anode operating conditions

Aitor Hornes (1), Martina Torchietto (1), Guttorm Syvertsen-Wiig (2), Rémi Costa (1)
(1) German Aerospace Centre (DLR), Institute of Technical Thermodynamics,
Pfaffenwaldring 38-40, 70569 Stuttgart, Germany
(2) CerPoTech AS, Kvenildmyra 6, 7072 Heimdal, Norway
Tel.: +49-711-6862-8116
Fax: +49-711-6862-747
aitor.hornesmartinez@dlr.de

Abstract

This work investigates the impact of the exposition to SOFC anode operating conditions on $SrTiO_3$-based compounds, with A-site or B-site substitution: 10 at.% lanthanum or 20 at.% niobium, respectively. Structural and surface stability of the materials after the reaction was examined (post-mortem analysis) using X-ray diffraction (XRD) and X-ray photoelectron spectroscopy (XPS). These techniques have allowed us to obtain bulk and surface information of the samples which will have a crucial relevance in revealing possible modifications accomplished during system operation. These modifications could play an important role in the degradation of the cell.
Structural analysis of materials before and after reduction did not show the formation of secondary phases, indicating a good stability of their crystalline structures for both samples under the conditions employed. In turn, surface study by means of XPS evidenced a surface enrichment in strontium oxide species for raw samples just after annealing. Nevertheless, exposure to the reducing environment caused an accumulation on the surface of the cations that occupy B positions in the perovskite structure oxides. At the same time, lanthanum segregation to the surface after the exposition to the reducing treatment was revealed as well. Achieved identification of the cationic diffusion processes that happened throughout cell operation will help us to understand and eventually minimize the degradation of the anode materials.

Introduction

Ni/YSZ cermets are the most common materials in the SOFC anode context. They have been widely preferred due to their high ionic and electronic conductivity, mechanical stability and excellent chemical and thermal compatibility with the most common electrolytes (YSZ, CGO) [1,2,3]. In these materials, Ni presence provides not only electronic conductivity but catalytic activity as well [1,2,3]. Although they have shown an excellent performance under ideal operating conditions, i.e. using "clean" H_2 as fuel and neither thermal nor redox events occurring, several drawbacks directly associated with Ni presence in the anode have been detected when more realistic conditions, such as the use of hydrocarbon-based fuels (e.g. syngas, biogas, etc.), presence of pollutants (e.g. S, PH_3), thermal cycling, etc., are employed that might lead to the irreversible degradation of the fuel cell [1,2,3]. Consequently, substitution of Ni by an alternative material in SOFC anodes has become a topic of imperative relevance for the development of SOFC technology. In this sense, perovskite-based materials, with general formula ABO_3, have shown promising results under anodic operating conditions which have made them attractive for their application as fuel electrodes in SOFC. Main advantages of perovskite oxide materials are their thermal, redox and mechanical stability and physical compatibility with electrolytes [4]. Moreover, they show a relatively flexible structure which tolerates extensive cationic substitution at two different available crystallographic positions [5]. This characteristic allows tuning up anodic materials properties to a great extent. Within this group of materials, some of the most promising are based on strontium titanates in which different cations, such as La^{3+}, Y^{3+} or Nb^{5+}, have been incorporated in the perovskite structure. During operation these materials have exhibited relatively high values of electrical conductivity and good chemical compatibility with other cell components [6,7,8]. One of their major drawbacks is the lack of catalytic activity towards fuel oxidation [9] and the addition of catalysts is necessary in order to improve their performance. Stability under operating conditions is another key factor that SOFC anode materials must face. In the case of perovskite-based anodes, degradation phenomena will likely involve diffusion/migration of atoms through the structure, which could result in the formation of undesired phases that would affect the performance and/or the integrity of the cell [10]. Due to that, a detailed study of the evolution of the materials in such severe conditions is necessary.

In this context, the present contribution analyses the structural and chemical stability of two perovskite-based oxides. Lanthanum or niobium-substituted strontium titanates were chosen for evaluating their stability when they are employed as SOFC anodes.

1. Experimental

Powders used in this investigation: $SrTi_{0.8}Nb_{0.2}O_3$ (hereafter STN) and $La_{0.1}Sr_{0.9}TiO_3$ (hereafter LST) were supplied by SAAN Innovation (Sweden) and CerPoTech AS (Norway), respectively.

Structural stability of the materials after exposure to reducing environment was analysed by means of X-ray diffraction (XRD). For this test raw powders were compressed using a uniaxial press to create pellets. Afterwards, samples were exposed to a reducing atmosphere (100% H_2) at 990ºC for 50h. For this treatment a cold-wall retort furnace Nabertherm VHT 40/16MO H_2 was employed. In this furnace H_2 atmosphere is purged 4

times per hour and refill with new H_2 each time. On the other hand, for the analysis of the surface "post-mortem" samples obtained after electrochemical testing were employed. For this purpose, electrolyte-supported cells were prepared by wet powder spraying. For preparing the full cells, YSZ commercial substrates (Kerafol, 150 μm thick, 48 mm dia.) were sprayed with an ethanol-based suspension containing the powder (LST or STN), DOLAPIX ET 85 (Zschimmer & Schwarz) as dispersant, PEG 400 (Sigma Aldrich) as plasticizer and Butvar® B-98 (Sigma Aldrich) as binder. Subsequently, on the other side of the electrolyte a $La_{0.8}Sr_{0.2}MnO_3$ (LSM, Fuel Cell Materials) and Yttria-stabilized zirconia (YSZ, Tosoh) ink vector (ratio 1:1 in volume, 70% of powders and 30% of ink in weight) was painted and fired to function as the cathode layer. Reducing treatment attained during electrochemical testing of the cells was characterized by 140 hours in contact with dry H_2 (H_2 conc. ≥ 50% vol., N_2 was used as diluent) and 8-16 hours at 980°C as maximum temperature.

Structural analysis was carried out by X-ray diffractometry using a Bruker D8 Discover diffractometer with VanTEC 2000 Detector System and Cu source. Exposures were made on reflection mode with a tuned monochromatic and parallel X-ray beam (Cu Kα), with an aperture of 1mm. The accelerating voltage was 45 kV and the tube current was 0.650 mA. Each diffraction pattern was measured in 4 frames with a step of 23°, starting with $\theta_1 = \theta_2 = 12°$ (Bragg-Brentano condition). The exposure time for each frame was 180 s.

Surface analysis was conducted by X-ray photoelectron spectroscopy (XPS). XPS experiments were performed using a Thermo ESCALAB 250 (Thermo Electron Corporation, East Grinstead, West Sussex, UK) UHV facility with a base pressure of 1×10^{-9} mbar. For XPS analysis of large surface areas (better statistics), a non-monochromatic Al twin-anode X-ray source (Thermo XR4) was used, operated at 300 W in combination with a hemispherical six channeltron electron energy analyzer operated in a large area mode (12.5 mm^2 analyzed surface area). For charge compensation, a Thermo FG01 (Thermo Electron Corporation, East Grinstead, West Sussex, UK) flood gun (25 μA emission at 5 eV) was used. Ion etching experiments (sputter yields not calibrated, Ion etching and tape peel-off depth profiling section) are performed by subsequent Ar+-sputtering (2 kV, 0.2 μA/μm2) and XPS analysis using the nonmonochromated X-ray source and a Thermo EX05 (Thermo Electron Corporation, East Grinstead, West Sussex, UK) ion gun.

2. Results

Figure 1 shows the X-ray diffractograms of STN and LST obtained before and after the reduction, respectively. Every sample showed a single phase characteristic cubic tausonite-type crystalline structure with crystallite sizes in the range of 30-40 nm. After 50 hours of reducing treatment, no additional peaks attributable to the formation of secondary phases were detected which indicates a good structural stability in agreement with reference works using similar materials [11,12,13]. Nevertheless, differences in the lattice parameter of the samples before and after the reducing treatment were observed. First, it is noteworthy to mention that addition of aliovalent cations (La or Nb) to the strontium titanate structure produced shrinkage or expansion of the crystal lattice, respectively, due to the different ionic radii of the added cations with respect to the ones present in the basic $SrTiO_3$ structure (a=3.9040 Å) [11].

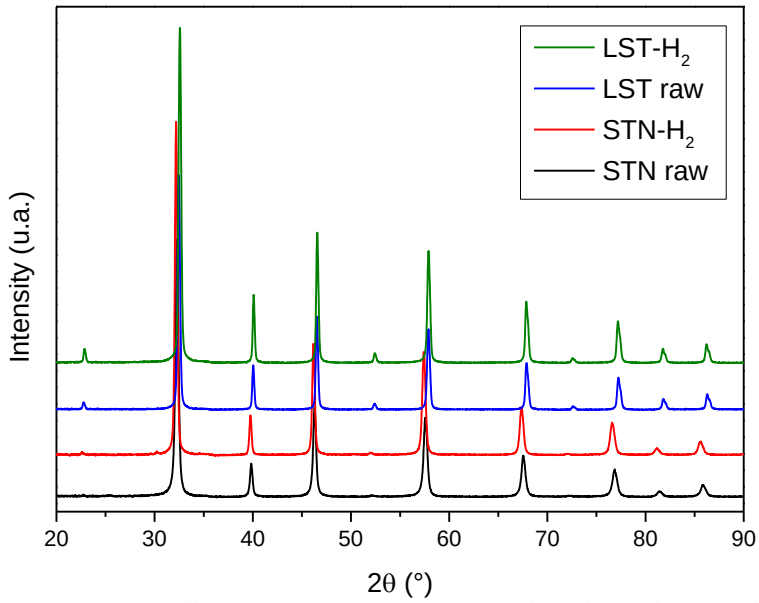

Figure 1: X-ray diffractograms of raw and reduced materials.

After the reducing treatment, both materials experienced an expansion associated most presumably with the presence of redox-active species in accordance with reported literature [11,12,13]. In principle, titanium and/or niobium could participate in this process due to their multiple oxidation states. Actually, looking at the values shown in Table 1, a larger increase for STN lattice parameter upon reaction is observed (127 Å for STN and 106 Å for LST), indicating a greater extent of the reduction process that could mean the participation of both elements, i.e. Ti and Nb. At this respect, Blennow et al. [14] evidenced that Nb is not affected by the reducing atmosphere. In fact, Chung et al. determined that Nb remains oxidized (oxidation state +V) even after being treated at 1360ºC for 20h in 100% H_2 [15]. Therefore, greater lattice expansion detected for reduced STN would be related only to Ti reduction.

Table 1: Lattice parameter (Å) for raw and reduced samples.

	Raw	Reduced
STN	3.9171	3.9298
LST	3.9040	3.9146

Subsequently, modifications occurred on the samples surface after the reaction will be discussed. Figure 2 shows the surface high resolution XPS spectra of Ti2p obtained for the samples. In these spectra, two main bands centered at ca. 458.7 eV and ca. 464.3 eV are identified. They correspond to the $Ti2p_{3/2}$ and $Ti2p_{1/2}$ spin-orbital splitting. The position occupied by the main contribution and the value of the splitting, ca. 5.6 eV, indicates the presence of titanium oxide on the surface. For reduced samples, Ar^+ sputtering was used for 5 seconds in order to remove the oxide layer formed on the surface due to ambient exposition. Such low sputtering time was chosen to avoid possible modifications in the chemical state of the species induced by the ion bombardment [16]. In these spectra, $Ti2p_{3/2}$ resolves into two components according to the Voigt-fitted curves. The peak at the lowest binding energy that is centered at ca. 457.1 eV, is attributed to Ti_2O_3 [17] while the

main peak centered at ca. 458.7 eV is assigned to the Ti^{4+} as for the raw oxides. Comparison of the contributions attributed to Ti^{3+} species for both reduced samples reveals larger segregation of these species on LST surface: 15% vs. 8%, for LST and STN, respectively.

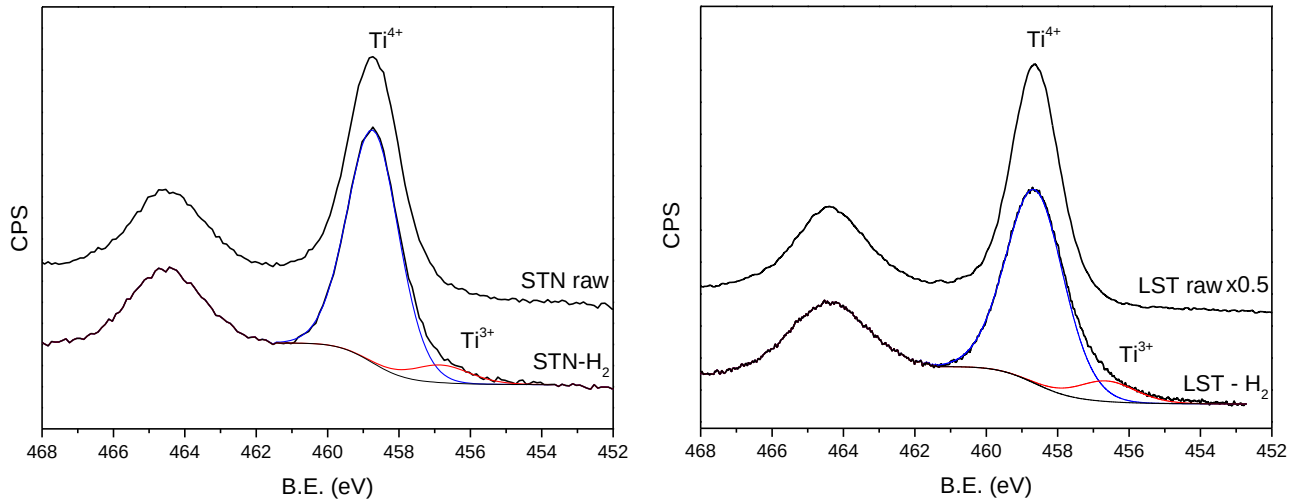

Figure 2: Ti2p XPS spectra for raw and reduced STN (left) and LST (right).

Regarding the redox behavior of niobium, surface analysis of Nb3d enables to detect a small contribution (< 5 at. %) at ca. 205 eV associated with NbO_x species, indicating a minor reduction of Nb after more than 100 h in reducing atmosphere at least on the surface, which is in agreement with Blennow and Chung's works [14,15].

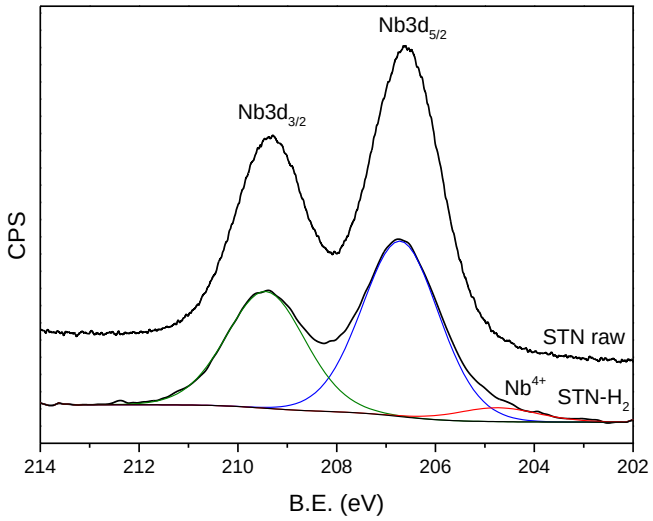

Figure 3: Nb3d XPS spectra for raw and reduced STN.

In Table 2 comparison between the atomic ratios of the different species before and after the reducing treatment is shown. Initially, the variation of the relation between the elements occupying the different cationic sites of the perovskite oxides (i.e. A-sites vs. B-sites) before and after the reducing treatment is examined. Bearing in mind that both

materials should have a nominal atomic ratio (A/B) of 1, the first aspect that we have to point out is the dramatic surface strontium enrichment shown by both oxides, more evident for the STN, just after annealing. This accumulation of SrO-enriched phases on the surface is related with the modification of the vacancy compensation mechanism under oxidizing atmospheres leading to the diffusion of Sr vacancies into the crystals [12]. In turn, excess of Sr species segregate to the surface and will be incorporated in Ruddlesden-Popper phases ($SrO{\cdot}nSrTiO_3$) in the near surface region and SrO_x phases on top of the surface [12]. This effect seems to be more prevalent while the dopant concentration increases which is in good accordance with the higher A/B atomic ratio observed for raw STN.

Table 2: Atomic ratios extracted of the XPS spectra.

STN			**LST**		
	Raw	Reduced		Raw	Reduced
Sr/(Ti+Nb)	1.90	1.31	**(La+Sr)/Ti**	1.66	1.33
Nb/Ti	1.04	0.99	**La/Sr**	0.03	0.10

Analysis of the same parameter after the reaction showed a decrease of this value which suggests a surface enrichment on B-site cations. This phenomenon has been described by Neagu et al. [18] and can be used to tailor the surface of perovskite-based materials with a desired element. Finally, differences in the behavior of the aliovalent cations added, Nb and La, were observed as well. While Nb/Ti (B'/B'') ratio remained almost constant, La segregates to the surface in great extent.

Conclusion

Structural and chemical modifications occurred under operating conditions for two alternative SOFC anodes based on perovskite structure materials have been evaluated. Lanthanum or niobium-substituted strontium titanates were exposed to highly reducing environment. Evaluation of materials structure and surface composition before and after this treatment has been carried out. Although no evidence of structural changes has been identified, surface alterations have been detected. Compositional differences found on the samples surface between the stoichiometric value and the real shown indicate the importance of the heritage received from previous treatments that the samples have suffered, e.g. in the annealing stage. Even though the materials are chemically different in terms of addition of different aliovalent cations, substitution in different cationic position and amount of aliovalent element incorporated; both samples experienced similar enrichment of their surfaces by B-site cations during the reducing treatment. Moreover, segregation of La to the surface was observed as well even if it is occupying A-site positions in the perovskite structure.

Modifications revealed by this work arisen during the reaction might be prone to cause undesired effects which could lead to the failure of the system. In this case, changes in the crystallographic structure have not been detected, but more detailed surface study have shown several variations that need further investigation in order to minimize degradation phenomena of these materials under operation.

References

[1] W.Z. Zhu, S.C. Deevi, A review on the status of anode materials for solid oxide fuel cells, Mater. Sci. Eng. A362 (2003) 228
[2] S.P. Jiang, S.H. Chan, A review of anode materials development in solid oxide fuel cells, J. Mater. Sci. 39 (2004) 4405.
[3] J.B. Goodenough, Y-H. Huang, Alternative anode materials for solid oxide fuel cells, J. Power Sources. 173 (2007) 1.
[4] E.V. Tsipis, V.V. Kharton, Electrode materials and reaction mechanisms in solid oxide fuel cells: a brief review. I. Performance-determining factors, J. Solid State Electrochem. 12 (2008) 1039.
[5] J.T.S. Irvine, Perovskite for SOFC anodes oxides, in Perovskite oxides for solid oxide fuel cells, T. Ishihara, ed., Springer, ISBN 978-0-387-77707 - 8 (2009) 168.
[6] P.R. Slater, D.P. Fagg, J.T.S. Irvine, Synthesis and electrical characterisation of doped perovskite titanates as potential anode materials for solid oxide fuel cells, J. Mater. Chem., 7 (1997) 2495.
[7] S.Q. Hui, A. Petric, Evaluation of yttrium-doped $SrTiO_3$ as an anode for solid oxide fuel cells J. Euro. Ceram. Soc. 22 (2002) 1673.
[8] O.A. Marina, N.L. Canfield, J.W. Stevenson, Thermal, electrical, and electrocatalytic properties of lanthanum-doped strontium titanate, Solid State Ionics 149 (2002) 21.
[9] S. Lee, G. Kim, J.M. Vohs, R.J. Gorte, SOFC Anodes Based on Infiltration of $La_{0.3}Sr_{0.7}TiO_3$, J. Electrochem. Soc. 155 (2008) B1179.
[10] M.A. Pena, J.L.G. Fierro, Chemical Structures and Performance of Perovskite Oxides, Chem. Rev. 101 (2001) 1981.
[11] J.T.S. Irvine, P.R. Slater, P.A. Wright, Synthesis and Electrical Characterisation of the Perovskite Niobate-Titanates $Sr_{1-x/2}Ti_{1-x}Nb_xO_3$, Ionics 2 (1996) 213.
[12] R. Moos, K.H. Härdtl, J. Am. Ceram. Soc. 80 (1997) 2549.
[13] J. Karczewski, B. Riegel, M. Gazda, P. Jasinski und B. Kusz, J. Electroceram. 24 (2010) 326.
[14] P. Blennow, a Hagen, K. Hansen, L. Wallenberg, and M. Mogensen, Defect and electrical transport properties of Nb-doped $SrTiO_3$, Solid State Ionics. 179 (2008) 2047.
[15] S. Chung, S. L. Kang, and V. P. Dravid, Effect of Sintering Atmosphere on Grain Boundary Segregation and Grain Growth in Niobium-Doped $SrTiO_3$, J. Am. Ceram. Soc. 10 (2002) 2805.
[16] S. Hashimoto, Ch. Tanaka, A. Murata, T. Sakurada, Formulation for XPS Spectral Change of oxides by Ar Ion Bombardment: Application of the Formulation to Ta2O5 System, J. Surf. Anal. 13 (2006) 14.
[17] M.C. Biesinger, L.W.M. Lau, A.R. Gerson, R.St.C. Smart, Resolving surface chemical states in XPS analysis of first row transition metals, oxides and hydroxides: Sc, Ti, V, Cu and Zn, Appl. Surf. Sci. 257 (2010) 887.
[18] D. Neagu, G. Tsekouras, D.N. Miller, H. Menard, J.T.S. Irvine, In situ growth of nanoparticles through control of non-stoichiometry, Nature Chem. 5 (2013) 916.